Configuring Au and Ag nanorods for sensing applications

Ovidio Peña-Rodríguez,[1,*] Umapada Pal,[2] Vladimir Rodríguez-Iglesias,[3] Luis Rodríguez-Fernández,[3] and Alicia Oliver[3]

[1]*Institut de Ciencia de Materials de Barcelona (ICMAB-CSIC), Campus UAB, Bellaterra, Barcelona 08193, Spain*
[2]*Instituto de Física, Universidad Autónoma de Puebla, Apartado Postal J-48, Puebla, Puebla 72570, Mexico*
[3]*Instituto de Física, Universidad Nacional Autónoma de México, Apartado Postal 20-364, Mexico City 01000, Mexico*
**Corresponding author: ovidio@bytesfall.com*

Received November 22, 2010; revised January 11, 2011; accepted January 12, 2011; posted January 20, 2011 (Doc. ID 138416); published March 14, 2011

We have studied optimum configurations of Au and Ag nanorods for optical sensing applications. From the analysis of the resonance condition by means of the quasistatic approximation, it was found that sensitivity is controlled by two main factors: the aspect ratio of the nanorods and their composition (the metal's bulk plasma wavelength), and it depends linearly on both. The finding was confirmed quantitatively using T-matrix calculations, even for particles with a radius of 40 nm, where the quasistatic approximation is no longer valid. For ease of detection, the intensity of the surface plasmon resonance band of the nanostructures was included along with its full-width at half-maximum in the correction factor C, which on multiplying with the sensitivity ($\Delta\lambda_{\mathrm{SPR}}/\Delta n_m$) gives a figure of merit. It has been demonstrated that the metal nanorods, especially the larger ones, have better optical sensitivity than the nanostructures of nanobox- or nanoshell-like geometries, which have been reported to be the best optical sensors for these metals.

OCIS codes: 050.6624, 160.3900, 160.4236, 160.4760, 240.6680.

1. INTRODUCTION

Potential applications of metal nanoparticles (NPs) in areas such as chemical and biochemical sensing [1,2] or cancer treatment [3] arising from the dependence of their surface plasmon resonance (SPR) frequency on the refractive index of the surrounding environment [4] have made them the subject of intensive research nowadays [5,6]. For sensing applications, a high sensitivity of the SPR frequency to the change in the refractive index of the surroundings ($\Delta\lambda_{\mathrm{SPR}}/\Delta n_m$) is required. However, the plasmonic behaviors of metal NPs and their sensitivity to the refractive index change of the embedding medium strongly depend on their physical geometry. Numerous studies have been performed [7–12] on metallic nanostructures of various geometries to find suitable configurations with optimum sensitivity. Nevertheless, it has been noticed that not only the sensitivity of the SPR band of the NPs matters for sensing applications, but also its width, as this parameter affects ease of detection [9,12,13]. For that very reason, a figure of merit (FOM) was defined [12] by multiplying the sensitivity by a correction factor C, which is related to the full-width at half-maximum (FWHM) of the plasmon band through the relation: $C = 1/\mathrm{FWHM}$. Using this expression of FOM, it has been claimed that nanocubes [12] and nanoboxes [10] (hollow nanocubes) are the most efficient metallic NPs for sensing applications. However, even though there has been no shortage of efforts to use metallic nanorods as sensors [14–16], none of the reported works have taken this correction factor into account while estimating their sensitivity.

A simple yet effective way to represent the nanorods is through prolate spheroids, which can be formed by rotating an ellipse around its major axis. They can be described with two parameters: b, which is the rotational (transversal) semiaxis, and a, the longitudinal semiaxis. However, it is more convenient to describe their shape using the aspect ratio ϵ (the ratio of the longitudinal to the rotational axis, a/b) and their size using the radius r_V of a sphere having the same volume. The typical single SPR peak observed for a sphere is split in two for the nanospheroids, i.e., the longitudinal and transverse modes, which are red- and blueshifted, respectively. This effect can be explained by the presence of a high density of electronic charge at the spheroid extremity, produced by polarization. Therefore, a greater (lower) electron screening occurs in the longitudinal (transverse) direction, resulting in a weaker (stronger) restoring force of the electron gas, and therefore lowering (increasing) its resonance frequency.

In this work, we have studied the dependence of the refractive index sensitivity and SPR bandwidth on the aspect ratio of gold and silver prolate spheroids in random orientations (Fig. 1), using T-matrix calculations [17], to find their optimum configurations for sensing applications. For the calculations we used the free code developed by Mishchenko and Travis [18]. The bulk dielectric function values of gold and silver reported by Johnson and Christy [19] were used after a correction to incorporate the surface dispersion effects [20]. It has been demonstrated that these metallic nanorods with optimum aspect ratios have excellent sensitivity, even surpassing that of other more exotic geometries, which are harder to synthesize.

2. T-MATRIX METHOD

The T-matrix method was originally developed by Waterman [21] and later improved by Mishchenko *et al.* and Wielaard *et al.* [22–24]. In this method, the incident, internal, and

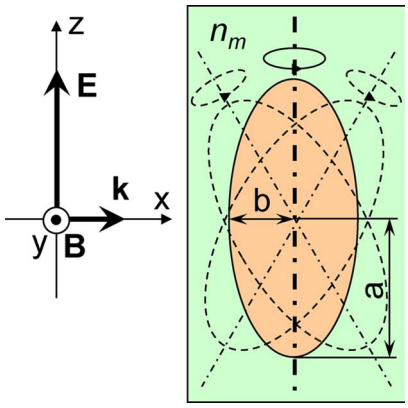

Fig. 1. (Color online) Schematic representation of a randomly oriented prolate spheroid, showing the impinging electromagnetic waves. **E** and **B** are the electric and magnetic fields, respectively, and **k** is the wave vector.

scattered electric fields ($\vec{E}_i$, $\vec{E}_{\text{int}}$, and $\vec{E}_s$) are expanded in terms of appropriate sets of spherical wave functions, which are correlated by means of a transition (or T) matrix. A relation between the expansion coefficients for the incident and the scattered fields can be obtained by using integral representations of the electric fields, which should satisfy the vector Helmholtz equation:

$$\nabla \times \nabla \times \vec{E} - k^2 \vec{E} = 0 \qquad (k = 2\pi/\lambda), \tag{1}$$

where λ is the wavelength in the medium. The best basis functions for a spheroidal particle are spherical wave vectors, $\vec{M}_\upsilon$ and $\vec{N}_\upsilon$; υ represents the spherical harmonic double index m and n. When the time dependence $\exp(-i\omega t)$ is used ($\omega = kc$ and c is the speed of light), these functions are given by

$$\vec{M}_\upsilon = \nabla \times \vec{r} \cdot \exp(-im\varphi) P_n^m(\cos(\theta)) \times [j_n(kr) + in_n(kr)], \tag{2a}$$

$$\vec{N}_\upsilon = k^{-1} \nabla \times \vec{M}_\upsilon, \tag{2b}$$

with the geometric parameters defined following Mishchenko *et al.* [17]. Here $P_n^m(\cos(\theta))$ are the associated Legendre functions, $j_n(kr)$ are the spherical Bessel functions, $n_n(kr)$ are the Neumann functions, and the indices are $n = 0, 1, \ldots..;$ $m = -n, -n+1, \ldots..., n-1, n$. These functions are outward traveling waves with singularity at the origin that satisfy the Helmholtz vector equation and form a complete set of functions on the unit sphere. The corresponding functions that are regular (finite) at the origin are obtained by excluding the Neumann function $n_n(kr)$ from Eq. (2). Thus, the regular vector waves, $\vec{M}_\upsilon^r$ and $\vec{N}_\upsilon^r$, have a pure Bessel function radial dependence. The incident field in the surrounding medium is regular at the origin, and thus can be expanded as regular waves such as

$$\vec{E}_i(k_{\text{med}}\vec{r}) = E_0 \sum_\upsilon D_\upsilon [a_\upsilon \vec{M}_\upsilon^r(k_{\text{med}}\vec{r}) + b_\upsilon \vec{N}_\upsilon^r(k_{\text{med}}\vec{r})], \tag{3}$$

where E_0 is the amplitude of the incident field, D_υ is a normalization constant, a_υ and b_υ are the expansion coefficients that are assumed to be known, and for an incident plane wave, they are expressed in terms of the associated Legendre functions and their derivatives [21]. The internal field can be expanded in terms of the same regular waves:

$$\vec{E}_{\text{int}}(k_{\text{part}}\vec{r}) = E_0 \sum_\mu [c_\mu \vec{M}_\mu^r(k_{\text{part}}\vec{r}) + d_\mu \vec{N}_\mu^r(k_{\text{part}}\vec{r})], \tag{4}$$

where μ incorporates the two spherical harmonic indices mentioned above and c_μ and d_μ are the expansion coefficients of the internal field. Finally, the outgoing scattered field can be expressed in terms of outgoing spherical waves [by keeping the Neumann function in Eq. (2)]:

$$\vec{E}_s(k_{\text{med}}\vec{r}) = E_0 \sum_\upsilon D_\upsilon [f_\upsilon \vec{M}_\upsilon^o(k_{\text{med}}\vec{r}) + g_\upsilon \vec{N}_\upsilon^o(k_{\text{med}}\vec{r})], \tag{5}$$

where f_υ and g_υ are the expansion coefficients characterizing the scattered field. They are obtained by multiplying the known expansion coefficients of the incident field by a so-called transition matrix or T matrix:

$$\begin{bmatrix} f_\upsilon \\ g_\upsilon \end{bmatrix} = \begin{bmatrix} T^{11} & T^{12} \\ T^{21} & T^{22} \end{bmatrix} \begin{bmatrix} a_\upsilon \\ b_\upsilon \end{bmatrix}. \tag{6}$$

Equation (6) is the main equation of the T-matrix approach; only the expansion coefficients of the incident field and the elements of the T matrix need to be calculated now.

Finally, Mishchenko's averaging scheme [25] was used to calculate the orientation averaging of the optical properties, because in most real systems the nanorods are randomly oriented. This method is very efficient in computational terms because the T matrix is calculated only once during averaging. This can be accomplished by taking advantage of the fact that the T matrix does not depend on the directions of propagation and the states of polarization of the incident and scattered fields, but only on the size, morphology, and composition of the scattering particle as well as on its orientation with respect to the laboratory reference frame.

3. QUASISTATIC APPROXIMATION

In this section we will use the quasistatic approximation to theoretically analyze the main factors affecting the spectral sensitivity of the SPR. Despite its simplicity, this approach is useful to qualitatively understand many phenomena related to light scattering by small particles. In this approximation, the absorption cross section of randomly oriented ellipsoids can be calculated as [9,26]

$$\sigma_{\text{abs}}(\omega) = \frac{V\epsilon_m^{3/2}}{3c} \sum_{i=1}^{3} L_i^{-2} \frac{\omega \epsilon_2}{[\epsilon_1 + \epsilon_m(L_i^{-1} - 1)]^2 + \epsilon_2^2}, \tag{7}$$

where V is the particle volume, c is the speed of light in vacuum, $\epsilon_{np} = \epsilon_1 + i\epsilon_2$ and ϵ_m are the dielectric functions of the NP and the surrounding medium, respectively, and L_i are geometric factors. For prolate spheroids, the L_i terms only depend on the eccentricity ($e = \sqrt{1 - (b/a)^2}$), through the relations [27]

$$L_1 = \frac{1 - e^2}{e^2} \left[-1 + \frac{1}{2e} \ln\left(\frac{1+e}{1-e} \right) \right], \qquad L_2 = L_3 = \frac{1 - L_1}{2}. \tag{8}$$

For the longitudinal SPR, we obtain the resonance condition for the minimum of the denominator; by assuming that ϵ_2 is

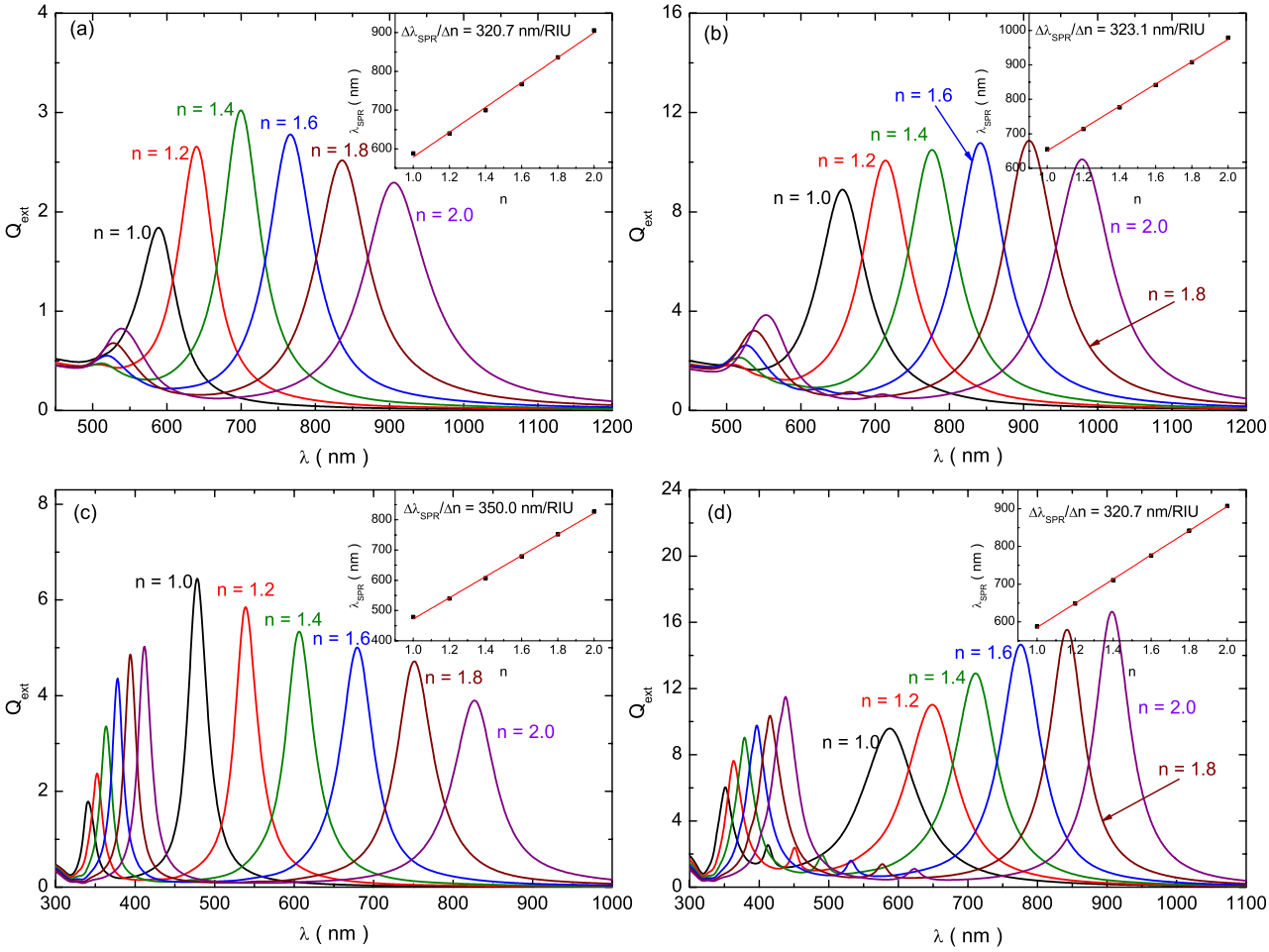

Fig. 2. (Color online) Simulated optical extinction spectra for gold (silver) prolate spheroids ($\epsilon = 3$), in random orientations, with equivalent radii of (a) [(c)] 10 and (b) [(d)] 40 nm, respectively, and embedded in different media with increasing refractive indices (1.0–2.0). The insets show the plots of the SPR peak position λ_{SPR} against the refractive index of the embedding medium. The solid lines are linear fits to the data points.

approximately constant (which is true in most cases), this condition can be simplified to $\epsilon_1 + \epsilon_m(L_1^{-1} - 1) = 0$. The dielectric function of the metal can also be approximated, by means of Drude's model [9,27]:

$$\epsilon_{np}(\omega) = \epsilon_{ib} - \frac{\omega_p^2}{\omega^2 - i\omega\Gamma} \approx \epsilon_{ib} - \frac{\omega_p^2}{\omega^2} + i\frac{\omega_p^2}{\omega^3}\Gamma, \tag{9}$$

where ω, ω_p, and Γ are the optical frequency, the metal plasma frequency, and the damping constant, respectively and ϵ_{ib} represents the interband contribution to the dielectric function. Now, using Eq. (9), the resonance condition can be rewritten as

$$\frac{\lambda_{\mathrm{SPR}}}{\lambda_p} = \frac{\omega_p}{\omega_{\mathrm{SPR}}} = \sqrt{\epsilon_{ib} + \epsilon_m(L_1^{-1} - 1)} = \sqrt{\epsilon_{ib} + n_m^2(L_1^{-1} - 1)}, \tag{10}$$

where λ_{SPR} and λ_p represent the SPR and the bulk plasma wavelengths, respectively, and n_m is the refractive index of the surrounding medium. Now, because the factor $L_1^{-1} - 1$ is approximately proportional to ϵ^2 ($L_1^{-1} - 1 \propto \epsilon^2$) [16], it follows that if ϵ_{ib} in Eq. (10) is small compared to the other term, then the sensitivity of the SPR wavelength to the refractive index variations is

$$\frac{d\lambda_{\mathrm{SPR}}}{dn_m} \propto \lambda_p\sqrt{L_1^{-1} - 1} \propto \epsilon\lambda_p. \tag{11}$$

It is clear from Eq. (11) that the sensitivity of the surface plasmon wavelength to the changes in refractive index of the local environment is linearly proportional to both λ_p (type of metal) and the aspect ratio of the nanorod. As for the widening of the SPR peak, it is first necessary to calculate the Taylor expansion of σ_{abs} near λ_{SPR} [28]:

$$\epsilon_1(\lambda) + \epsilon_m(L_i^{-1} - 1) \approx [\epsilon_1(\lambda_{\mathrm{SPR}}) + \epsilon_m(L_i^{-1} - 1)] + \left.\frac{\partial\epsilon_1(\lambda)}{\partial\lambda}\right|_{\lambda=\lambda_{\mathrm{SPR}}}(\lambda - \lambda_{\mathrm{SPR}}). \tag{12}$$

Now the FWHM of the SPR peak can be found from the analogy of the expression obtained for the absorption cross section with a Lorentzian function, after replacing the obtained expansion in Eq. (7) [28]:

$$\Delta\lambda_{1/2} = 2|\lambda_{\mathrm{SPR}} - \lambda_{1/2}| \approx 2\epsilon_2(\lambda_{\mathrm{SPR}})/\left|\left.\frac{\partial\epsilon_1(\lambda)}{\partial\lambda}\right|_{\lambda=\lambda_{\mathrm{SPR}}}\right|. \tag{13}$$

This equation shows that the width of the peak has a much more complex dependency on the parameters of the particle

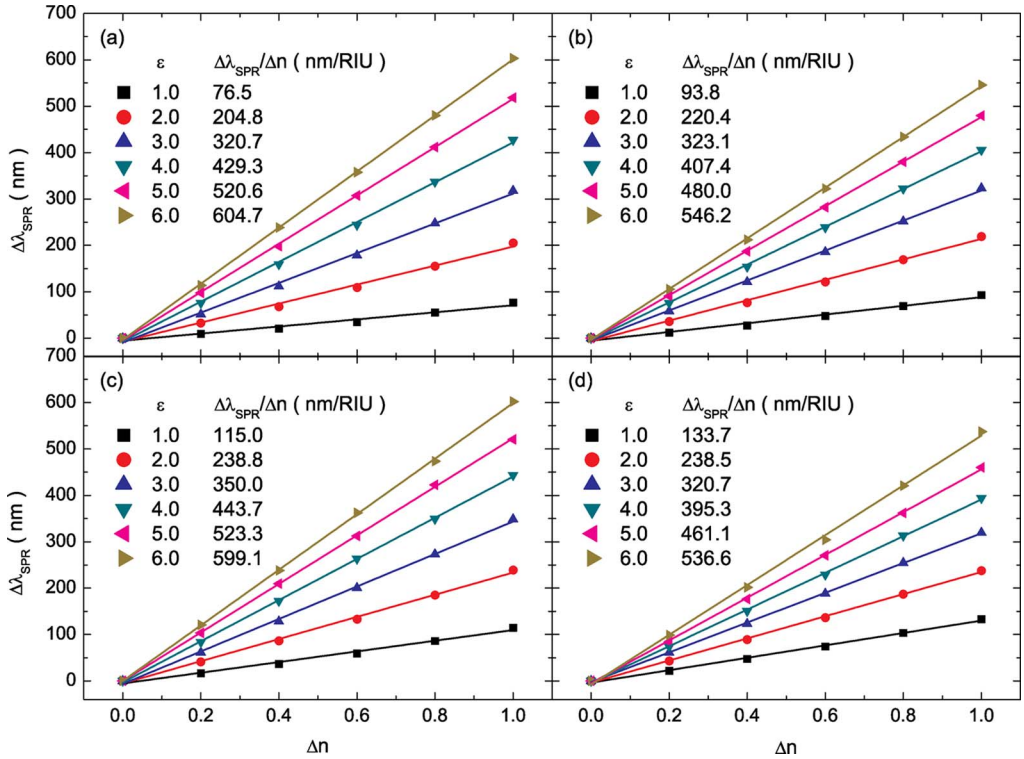

Fig. 3. (Color online) Change of SPR peak positions of gold (silver) nanorods of different aspect ratios ϵ, with equivalent radii of (a) [(c)] 10 and (b) [(d)] 40 nm, respectively, with the variation of the refractive index (n_m) of the embedding medium. The lines are linear regressions, used to obtain the reported sensitivities (slope of the lines).

than the sensitivity. However, Eq. (13) indicates that the bandwidth is narrower when the imaginary part of the dielectric function of the metal is smaller and the gradient of the real part is steeper.

In principle, Eqs. (11) and (13) are just rough approximations of the influence of the particles' parameters on the SPR sensitivity and linewidth, and they should be valid only for very small particles ($r_V < 10$ nm). However, we will demonstrate in the next section that they remain valid when the size of the NP is increased beyond this limit. For this, the results obtained by an exact method (T matrix) will be presented. The calculations will be performed for nanospheroids with radii of 10 nm (where the assumptions we made are mostly met) and 40 nm (where the quasistatic approximation is not valid).

4. RESULTS AND DISCUSSION

The calculated optical extinction spectra for randomly oriented gold and silver prolate spheroids, embedded in different media, with aspect ratio $\epsilon = 3$ and equivalent radii r_v of 10 nm and 40 nm are shown in Fig. 2. Regardless of size, an increase of the refractive index of the surrounding environment produced a redshift for both the SPR modes. The effect is more pronounced for the longitudinal mode than for the transversal mode. Therefore, all our subsequent discussions are restricted to the former mode. As can be seen (insets of Fig. 2), the shift of the SPR position is linear for both the metals. A linear regression of the SPR wavelengths yielded similar experimental sensitivities of the small (big) NPs to the refractive index variations ($\Delta\lambda_{\mathrm{SPR}}/\Delta n_m$): 320.7 and 350.0 (323.1 and 320.7 nm) per refractive index unit (RIU) for gold and silver, respectively. Those values are equivalent or better than the ones reported for some other shapes such as nanoboxes [10] and nanoshells [29,30] of the same metals. Indeed, the sensitivity can be greatly improved by increasing the aspect ratio of the nanorods. For instance, when ϵ is varied from 1.0 to 6.0, the $\Delta\lambda_{\mathrm{SPR}}/\Delta n_m$ of gold (silver) spheroids changes from 76.5 to 604.7 nm/RIU (115.0 to 599.1 nm/RIU) and from 93.8 to 546.2 nm/RIU (133.7 to 536.6 nm/RIU) for the small (10 nm) and big (40 nm) particles, respectively, as shown in Fig. 3.

However, the enhancement of the sensitivity does not come without a cost, because the linewidth (FWHM) of the SPR peak also becomes larger on increasing the aspect ratio (Fig. 4). Moreover, the increase of the FWHM with the aspect ratio is more pronounced than that of the sensitivity for the corresponding nanostructure [Fig. 5(a); the plotted values correspond to the average FWHM, because it also depends on the refractive index of the matrix]. From the plot of the FOM [Fig. 5(b)], it is clear that there is an optimum value of ϵ (between 3 and 4 for both metals) that yields a maximum sensitivity, which is comparable to the one reported by Cao *et al.* [10] for gold nanoboxes. Additionally, the small difference in sensitivity between gold and silver is considerably accentuated when it is taken into consideration that the latter metal has a much narrower plasmon than the former. Another effect, which is true in both cases but is much more evident for silver, is that the larger spheroids have worse FOM values than the smaller ones; this can be attributed to the broadening caused by the phase retardation effect [14]. Finally, it can be noted that the obtained values for the FOM are better than those reported for gold nanoboxes [10] and silver nanocubes [12].

So far we have shown that for sensing (optical and biological) applications, Au and Ag nanorods can compete

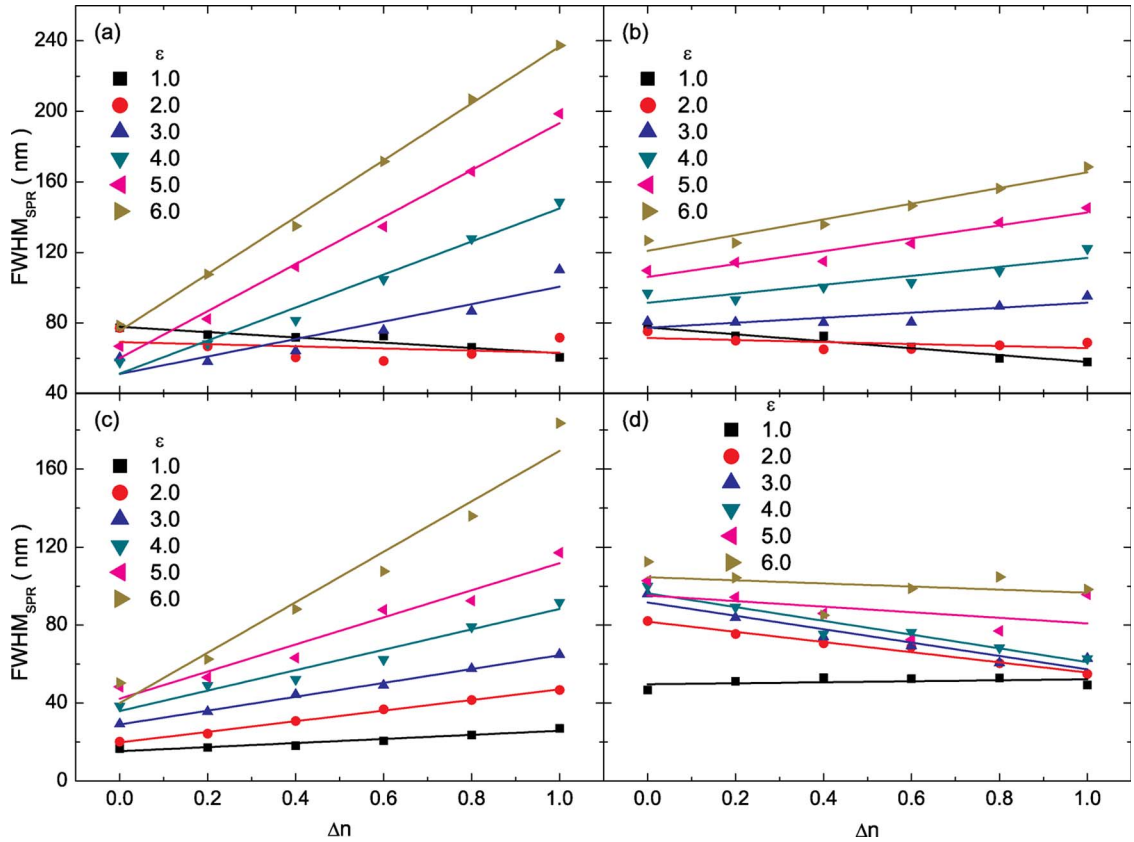

Fig. 4. (Color online) Variations of plasmon linewidth for gold (silver) nanorods of different aspect ratios ϵ, with equivalent radii of (a) [(c)] 10 and (b) [(d)] 40 nm, respectively, with the variation of the refractive index (n_m) of the embedding medium. The lines are a guide for the eye.

favorably with most of the geometric variants. However, it is worth examining an additional factor that makes them even more attractive. Apart from the linewidth, the intensity of the SPR peak of the metallic nanostructures is another factor that should also be taken into account for the ease of detection, for obvious reasons, of two peaks with the same linewidth, the more intense one would be easier to detect. Therefore, we propose to modify the correction factor to take into account the "slenderness" of the peak instead of just its linewidth. For the sake of simplicity, we assume that the SPR peak has a Lorenzian shape:

$$L_{\mathrm{SPR}} = \frac{Q_{\mathrm{ext}}^{\mathrm{SPR}}}{1 + \left(\frac{\lambda - \lambda_{\mathrm{SPR}}}{\mathrm{FWHM}/2}\right)^2}, \tag{14}$$

where $Q_{\mathrm{ext}}^{\mathrm{SPR}}$ is the extinction efficiency at the SPR wavelength; the correction factor now can be redefined as

$$C = \frac{\int_{-\infty}^{\infty} L_{\mathrm{SPR}} \mathrm{d}\lambda}{\mathrm{FWHM}} = \pi \frac{Q_{\mathrm{ext}}^{\mathrm{SPR}}}{\mathrm{FWHM}}. \tag{15}$$

In order to simplify the expression, the term π can be safely omitted from C (because it is a constant). It should be noted that both $Q_{\mathrm{ext}}^{\mathrm{SPR}}$ and the FWHM depend on the refractive index of the matrix and, therefore, their average values in the region of interest should be used. Finally, the new FOM can be rewritten as

$$\mathrm{FOM} = \frac{\langle Q_{\mathrm{ext}}^{\mathrm{SPR}} \rangle}{\langle \mathrm{FWHM} \rangle} \frac{\Delta \lambda_{\mathrm{SPR}}}{\Delta n_m}. \tag{16}$$

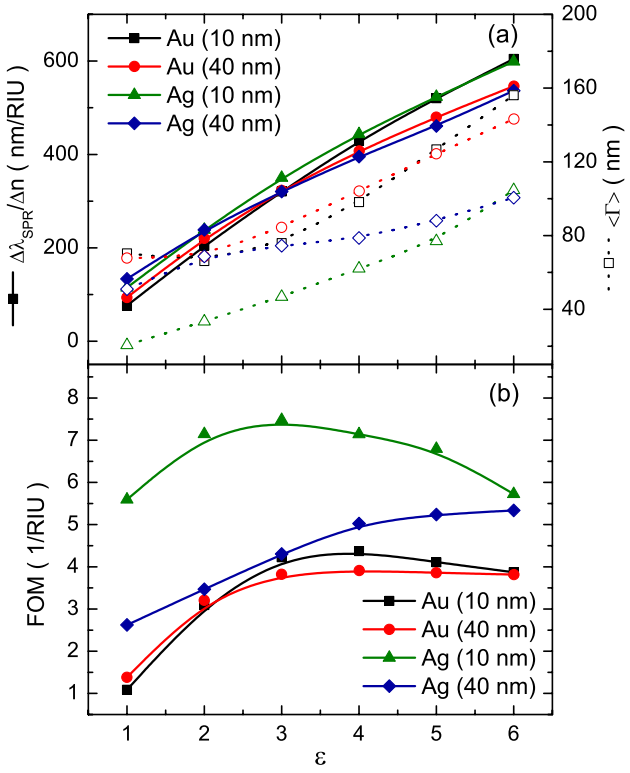

Fig. 5. (Color online) (a) Refractive index sensitivity $\Delta\lambda_{\mathrm{SPR}}/\Delta n_m$ (solid symbols), and FWHM (open symbols) of the SPR peak and (b) Sherry's FOM, plotted against the aspect ratio of gold [silver] nanorods, with equivalent radii of 10 (black squares) [(red circles)] and 40 nm (green triangles) [(blue diamonds)], respectively.

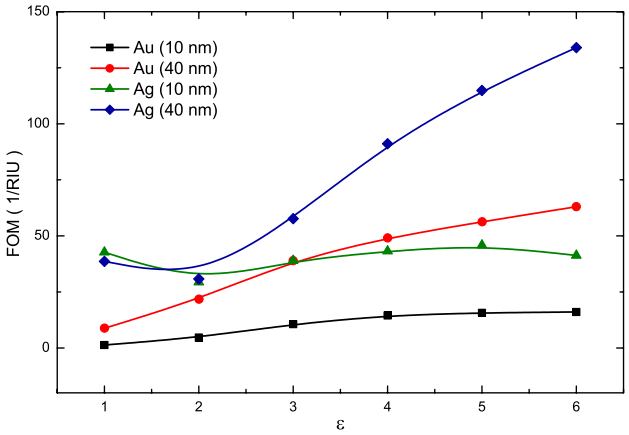

Fig. 6. (Color online) Amended FOM, plotted against the aspect ratio of gold (silver) nanorods, with equivalent radii of 10 (black squares) [(red circles)] and 40 nm (green triangles) [(blue diamonds)], respectively.

On increasing the aspect ratio of the metallic nanorods, their SPR gets more intense, unlike for nanoshells [31] and nanoboxes [10], where the intensity drops almost exponentially when the wall thickness is reduced. Therefore, the optical sensitivity of the nanorods with a proper aspect ratio is much higher than their nanoshell and nanobox counterparts. The FOM defined by Sherry *et al.* [12] does not take into account the effect of the intensity for the sake of ease of detection. Therefore, the FOM we defined in Eq. (16) should provide a more realistic assessment of the appropriateness of a structure to be used as a sensor. As an example, our newly defined FOM, calculated for the same types of metal particles previously analyzed, is presented in Fig. 6. As can be seen, the larger particles present higher values of the FOM due to their higher SPR intensity. At the same time, the optimum aspect ratios were shifted to higher values than those previously obtained.

5. CONCLUSIONS

Through theoretical analysis and T-matrix calculations of randomly oriented Au and Ag prolate spheroids, it has been shown that the optical sensitivity of these nanostructures strongly depends on their composition, size and aspect ratio. While the sensitivity of the nanostructures increases considerably with ϵ, the width of their SPR peak increases more rapidly, making them difficult to apply as sensors. Taking into account these two factors, a FOM [12] was calculated, showing that there exists a size-dependent optimum aspect ratio for each of these metals, which makes them more suitable for sensing applications. According to this concept of the FOM, smaller NPs are better for sensing applications. However, incorporating the SPR intensity factor to the conventional FOM, our amended FOM revealed just the opposite result, indicating that larger particles would be the better sensors due to their higher SPR peak intensity.

ACKNOWLEDGMENTS

V. Rodríguez-Iglesias is grateful to Dirección General de Estudios de Posgrado–Universidad Nacional Autónoma de México (UNAM) for financial support. O. Peña-Rodríguez thanks Dirección General de Asuntos del Personal Académido–UNAM and Institut de Ciencia de Materials de Barcelona–Consejo Superior de Investigaciones Científicas for extending a postdoctoral fellowship through the UNAM–Consejo Superior de Investigaciones Científicas agreement. This work was partially supported by the Consejo Nacional de Ciencia y Tecnología under grant 102937.

REFERENCES

1. P. Alivisatos, "The use of nanocrystals in biological detection," Nat. Biotechnol. **22**, 47–52 (2004).
2. Y. Sun and Y. Xia, "Increased sensitivity of surface plasmon resonance of gold nanoshells compared to that of gold solid colloids in response to environmental changes," Anal. Chem. **74**, 5297–5305 (2002).
3. L. R. Hirsch, R. J. Stafford, J. A. Bankson, S. R. Sershen, B. Rivera, R. E. Price, J. D. Hazle, N. J. Halas, and J. L. West, "Nanoshell-mediated near-infrared thermal therapy of tumors under magnetic resonance guidance," Proc. Natl. Acad. Sci. USA **100**, 13549–13554 (2003).
4. K. L. Kelly, E. Coronado, L. L. Zhao, and G. C. Schatz, "The optical properties of metal nanoparticles: the influence of size, shape, and dielectric environment," J. Phys. Chem. B **107**, 668–677 (2003).
5. W. L. Barnes, A. Dereux, and T. W. Ebbesen, "Surface plasmon subwavelength optics," Nature **424**, 824–830 (2003).
6. S. A. Maier, P. G. Kik, H. A. Atwater, S. Meltzer, E. Harel, B. E. Koel, and A. A. Requicha, "Local detection of electromagnetic energy transport below the diffraction limit in metal nanoparticle plasmon waveguides," Nat. Mater. **2**, 229–232 (2003).
7. A. D. McFarland and R. P. Van Duyne, "Single silver nanoparticles as real-time optical sensors with zeptomole sensitivity," Nano Lett. **3**, 1057–1062 (2003).
8. G. Raschke, S. Kowarik, T. Franzl, C. Sönnichsen, T. A. Klar, J. Feldmann, A. Nichtl, and K. Kürzinger, "Biomolecular recognition based on single gold nanoparticle light scattering," Nano Lett. **3**, 935–938 (2003).
9. K. Lee and M. A. El-Sayed, "Gold and silver nanoparticles in sensing and imaging: sensitivity of plasmon response to size, shape, and metal composition," J. Phys. Chem. B **110**, 19220–19225 (2006).
10. M. Cao, M. Wang, and N. Gu, "Optimized surface plasmon resonance sensitivity of gold nanoboxes for sensing applications," J. Phys. Chem. C **113**, 1217–1221 (2009).
11. G. Raschke, S. Brogl, A. S. Susha, A. L. Rogach, T. A. Klar, J. Feldmann, B. Fieres, N. Petkov, T. Bein, A. Nichtl, and K. Kurzinger, "Gold nanoshells improve single nanoparticle molecular sensors," Nano Lett. **4**, 1853–1857 (2004).
12. L. J. Sherry, S. Chang, G. C. Schatz, R. P. Van Duyne, B. J. Wiley, and Y. Xia, "Localized surface plasmon resonance spectroscopy of single silver nanocubes," Nano Lett. **5**, 2034–2038 (2005).
13. C. Sönnichsen, T. Franzl, T. Wilk, G. von Plessen, J. Feldmann, O. Wilson, and P. Mulvaney, "Drastic reduction of plasmon damping in gold nanorods," Phys. Rev. Lett. **88**, 077402 (2002).
14. E. S. Kooij and B. Poelsema, "Shape and size effects in the optical properties of metallic nanorods," Phys. Chem. Chem. Phys. **8**, 3349–3357 (2006).
15. J. Fu, B. Park, and Y. Zhao, "Nanorod-mediated surface plasmon resonance sensor based on effective medium theory," Appl. Opt. **48**, 4637–4649 (2009).
16. S. Link, M. B. Mohamed, and M. A. El-Sayed, "Simulation of the optical absorption spectra of gold nanorods as a function of their aspect ratio and the effect of the medium dielectric constant," J. Phys. Chem. B **103**, 3073–3077 (1999).
17. M. I. Mishchenko, L. D. Travis, and A. A. Lacis, *Scattering, Absorption, and Emission of Light by Small Particles*, 1st ed. (Cambridge University, 2002).
18. M. I. Mishchenko and L. D. Travis, "Capabilities and limitations of a current FORTRAN implementation of the *T*-matrix method for randomly oriented, rotationally symmetric scatterers," J. Quant. Spectrosc. Radiat. Transf. **60**, 309–324 (1998).
19. P. B. Johnson and R. W. Christy, "Optical constants of the noble metals," Phys. Rev. B **6**, 4370–4379 (1972).
20. H. Hövel, S. Fritz, A. Hilger, U. Kreibig, and M. Vollmer, "Width of cluster plasmon resonances: bulk dielectric functions and

chemical interface damping," Phys. Rev. B **48**, 18178–18188 (1993).
21. P. C. Waterman, "Symmetry, unitarity, and geometry in electromagnetic scattering," Phys. Rev. D **3**, 825–839 (1971).
22. M. I. Mishchenko and L. D. Travis, "T-matrix computations of light scattering by large spheroidal particles," Opt. Commun. **109**, 16–21 (1994).
23. M. I. Mishchenko, L. D. Travis, and A. Macke, "Scattering of light by polydisperse, randomly oriented, finite circular cylinders," Appl. Opt. **35**, 4927–4940 (1996).
24. D. J. Wielaard, M. I. Mishchenko, A. Macke, and B. E. Carlson, "Improved T-matrix computations for large, nonabsorbing and weakly absorbing nonspherical particles and comparison with geometrical-optics approximation," Appl. Opt. **36**, 4305–4313 (1997).
25. M. I. Mishchenko, "Light scattering by randomly oriented axially symmetric particles," J. Opt. Soc. Am. A **8**, 871–882 (1991).
26. S. Fedrigo, W. Harbich, and J. Buttet, "Collective dipole oscillations in small silver clusters embedded in rare-gas matrices," Phys. Rev. B **47**, 10706–10715 (1993).
27. C. F. Bohren and D. R. Huffman, *Absorption and Scattering of Light by Small Particles* (Wiley-Interscience, 1998).
28. W. C. Huang and J. T. Lue, "Quantum size effect on the optical properties of small metallic particles," Phys. Rev. B **49**, 17279–17285 (1994).
29. M. M. Miller and A. A. Lazarides, "Sensitivity of metal nanoparticle surface plasmon resonance to the dielectric environment," J. Phys. Chem. B **109**, 21556–21565 (2005).
30. P. K. Jain and M. A. El-Sayed, "Surface plasmon resonance sensitivity of metal nanostructures: physical basis and universal scaling in metal nanoshells," J. Phys. Chem. C **111**, 17451–17454 (2007).
31. O. Peña, U. Pal, L. Rodríguez-Fernández, and A. Crespo-Sosa, "Linear optical response of metallic nanoshells in different dielectric media," J. Opt. Soc. Am. B **25**, 1371–1379 (2008).